Molecular Biology of the Cell
Vol. 13, 4414–4428, December 2002

A Specific Structural Requirement for Ergosterol in Long-chain Fatty Acid Synthesis Mutants Important for Maintaining Raft Domains in Yeast

Marlis Eisenkolb,*† Christoph Zenzmaier,*† Erich Leitner,‡ and Roger Schneiter*§¶

Institute of *Biochemistry, and ‡Food-Chemistry and Technology, Graz University of Technology, A-8010 Graz, Austria, and §Department of Medicine, Division of Biochemistry, University of Fribourg, CH-1700 Fribourg, Switzerland

Submitted February 28, 2002; Revised August 23, 2002; Accepted September 13, 2002
Monitoring Editor: Howard Riezman

Fungal sphingolipids contain ceramide with a very-long-chain fatty acid (C26). To investigate the physiological significance of the C26-substitution on this lipid, we performed a screen for mutants that are synthetically lethal with *ELO3*. Elo3p is a component of the ER-associated fatty acid elongase and is required for the final elongation cycle to produce C26 from C22/C24 fatty acids. *elo3*Δ mutant cells thus contain C22/C24- instead of the natural C26-substituted ceramide. We now report that under these conditions, an otherwise nonessential, but also fungal-specific, structural modification of the major sterol of yeast, ergosterol, becomes essential, because mutations in *ELO3* are synthetically lethal with mutations in *ERG6*. Erg6p catalyzes the methylation of carbon atom 24 in the aliphatic side chain of sterol. The lethality of an *elo3*Δ *erg6*Δ double mutant is rescued by supplementation with ergosterol but not with cholesterol, indicating a vital structural requirement for the ergosterol-specific methyl group. To characterize this structural requirement in more detail, we generated a strain that is temperature sensitive for the function of Erg6p in an *elo3*Δ mutant background. Examination of raft association of the GPI-anchored Gas1p and plasma membrane ATPase, Pma1p, in the conditional *elo3*Δ *erg6*^{ts} double mutant, revealed a specific defect of the mutant to maintain raft association of preexisting Pma1p. Interestingly, in an *elo3*Δ mutant at 37°C, newly synthesized Pma1p failed to enter raft domains early in the biosynthetic pathway, and upon arrival at the plasma membrane was rerouted to the vacuole for degradation. These observations indicate that the C26 fatty acid substitution on lipids is important for establishing raft association of Pma1p and stabilizing the protein at the cell surface. Analysis of raft lipids in the conditional mutant strain revealed a selective enrichment of ergosterol in detergent-resistant membrane domains, indicating that specific structural determinants on both sterols and sphingolipids are required for their association into raft domains.

INTRODUCTION

Sphingolipids are ceramide-containing lipids that are highly enriched in the outer leaflet of the plasma membrane, where they exert both structural and signaling functions (for review see Dickson, 1998; Schneiter, 1999). In fungi, these lipids are composed of an inositolphosphate-containing hydrophilic head group bound to phytoceramide. The mammalian ceramide typically contains saturated acyl chains ranging from 16 to 24 carbon atoms in length (Gu *et al.*, 1997). The fungal ceramide, on the other hand, contains a saturated C26 very-long-chain fatty acid. Synthesis of this C26 acyl chain occurs by chain elongation of saturated long-chain fatty acids (C16/C18), a reaction that requires an ER-associated acyl chain elongation complex. Elo2p and Elo3p are two components of this complex (Oh *et al.*, 1997). They are presumed to catalyze the condensing reaction of the elongation cycle and exhibit slightly different substrate specificities. Although Elo2p elongates C16/C18 fatty acids to C22/C24, Elo3p is specifically required for the final elongation step from C22/C24 to C26. Cells with mutations in *ELO3* are viable but synthesize ceramide/sphingolipids with C22/C24 instead of the natural C26 fatty acid. Synthesis of the C24/C26 fatty acid is essential as an *elo2*Δ *elo3*Δ

DOI: 10.1091/mbc.E02–02–0116.
¶ Corresponding author. E-mail address: roger.schneiter@unifr.ch.
† Both authors contributed equally to this work.

double mutant is not viable (Oh *et al.*, 1997). The physiological significance of this particular fatty acid requirement of the fungal ceramide is unknown, but it is interesting to note that maturation of glycerophosphatidylinositol (GPI)-anchored proteins in yeast involves acyl chain remodeling reactions that serve to introduce a C26 fatty acid into glycolipid protein anchors, suggesting that the presence of C26 is of functional importance (Sipos *et al.*, 1997).

Synthesis of ceramide in mammals and yeast is confined to the ER membrane; subsequent maturation of ceramide to the more complex sphingolipids occurs upon transport to the Golgi apparatus (Levine *et al.*, 2000; Funato and Riezman, 2001). The mature sphingolipids are then transported to the plasma membrane, where they are highly enriched, and constitute ~30% of all the phosphate-containing lipids (Patton and Lester, 1991; Hechtberger *et al.*, 1994). In addition to sphingolipids, the plasma membrane contains high levels of sterols (Lange *et al.*, 1989; Schneiter *et al.*, 1999). These high levels of sterols and sphingolipids are generally believed to be important for reducing the permeability of the outer most membrane, thus protecting the cell against hostile environmental conditions.

Sterols have a high affinity for lipids containing saturated acyl chains, particularly ceramide (Sankaram and Thompson, 1990; Schroeder *et al.*, 1994). By restricting acyl chain mobility on ceramide, sterols induce the formation of dispersed liquid ordered phase domains, which are resistant to solubilization by detergents (for review see Brown and London, 2000; Rietveld and Simons, 1998). These sphingolipid/cholesterol-rich membrane domains have been proposed to serve as platforms/rafts for the lateral sorting of certain proteins, particularly for those containing a GPI anchor (Brown and Rose, 1992; Simons and Ikonen, 1997; Muniz and Riezman, 2000). Sterols and ceramides are both synthesized in the ER membrane, allowing for a possible early lipid-dependent segregation of proteins along the secretory pathway to the plasma membrane (Brown and Rose, 1992; Bagnat *et al.*, 2000).

Sterols are the product of a complex biosynthetic pathway with more than 20 distinct reactions. The sterol-specific part of this pathway starts by the condensation of farnesyl pyrophosphate to form squalene and, in fungi, ends with the synthesis of ergosterol. The early reactions of this 11-step conversion are essential. They involve cyclization of squalene to lanosterol and subsequent removal of three methyl groups. The enzymes that catalyze the last five steps of the pathway are nonessential. They serve to modify the basic sterol backbone by introduction of a methyl group at position 24 of the side chain (*ERG6*), isomerization of the double bond from position 8 to position 7 (*ERG2*), introduction of a second double bond in the B ring (*ERG3*), introduction of a double bond at position 22 of the side chain (*ERG5*), and reduction of the methylene bond originally present at position 24 (*ERG4*; see Figure 1A; for review see Lees *et al.*, 1999; Parks *et al.*, 1999).

Just as sphingolipids differ in structure between fungi and mammals, the sterols differ too. Ergosterol is distinct from the mammalian cholesterol by three structural modifications, two in the side chain and one in the B ring. The structure of the plant sterols is intermediate between that of the fungal ergosterol and the mammalian cholesterol. The

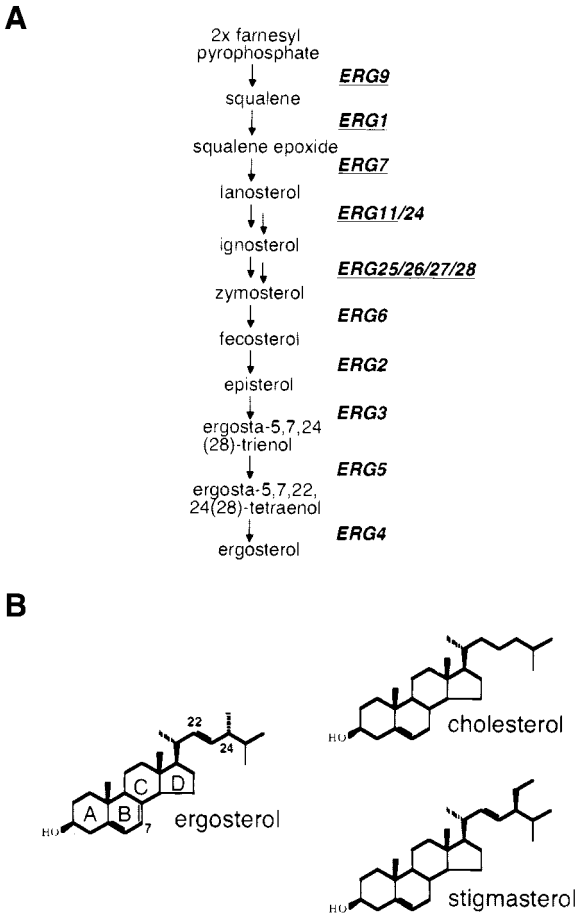

Figure 1. Outline of the sterol biosynthetic pathway in yeast and comparison of sterol structure from yeast, plants, and mammals. (A) Overview of the sterol-specific part of the ergosterol biosynthetic pathway. Essential enzymes are underlined. (B) Comparison of the structure of the major sterols from fungi, mammals, and plants. The yeast sterol, ergosterol, differs from the mammalian cholesterol by i) the presence of a methyl group at position 24, ii) an additional double bond at position 22, and iii) an additional double bond at position 7 of the B ring. The plant sterols stigmasterol and sitosterol have an ethyl group at position 24, a B-ring configuration as cholesterol and the presence (stigmasterol) or absence (sitosterol) of a double bond at position 22.

functional significance of these structural differences, however, is not yet understood (see Figure 1B).

We were interested in investigating the physiological role of the C26 substitution on the fungal ceramide. Using a screen for mutants that are synthetically lethal with *elo3*Δ, genetic conditions under which the final elongation step from C22/C24 to C26 becomes essential were generated. One of the mutants isolated in this screen is defective in the sterol C-24 methyltransferase, *ERG6* (Gaber *et al.*, 1989). We show here that the interaction between *ELO3* and *ERG6* is highly specific and affects raft structures at the plasma membrane, indicating that fungal-specific lipid modifications in sterols and sphingolipids are codependent and of functional significance.

Table 1. *S. cerevisiae* strains used in this study

Strain	Relevant genotype	Source or reference
FY1679	*MAT***a**/*MAT*α *TRP1/trp1*Δ*63 HIS3/his3*Δ*200 LEU2/leu2*Δ*1 ura3-52/ura3-52*	Winston *et al.* (1995)
FY1679a	*MAT***a** *his3*Δ*200 leu2*Δ*1 ura3-52*	Winston *et al.* (1995)
CH1462	*MAT*α *ade2 ade3 his3 leu2 ura3*	Kranz and Holm (1990)
RH2607	*MAT***a** *his4 leu2 ura3 bar1 lcb1-100,*	Sütterlin *et al.* (1997)
YRS1411	*MAT*α *his3*Δ*1 leu2*Δ*0 ura3*Δ*0 lys2*Δ*0 erg2*::*kanMX*	EUROSCARF; Winzeler *et al.* (1999)
YRS1256	*MAT*α *his3*Δ*1 leu2*Δ*0 ura3*Δ*0 lys2*Δ*0 erg3*::*kanMX*	EUROSCARF; Winzeler *et al.* (1999)
YRS1254	*MAT*α *his3*Δ*1 leu2*Δ*0 ura3*Δ*0 lys2*Δ*0 erg4*::*kanMX*	EUROSCARF; Winzeler *et al.* (1999)
YRS1253	*MAT*α *his3*Δ*1 leu2*Δ*0 ura3*Δ*0 lys2*Δ*0 erg5*::*kanMX*	EUROSCARF; Winzeler *et al.* (1999)
YRS1266	*MAT*α *his3*Δ*1 leu2*Δ*0 ura3*Δ*0 lys2*Δ*0 erg6*::*kanMX*	EUROSCARF; Winzeler *et al.* (1999)
YRS1410	*MAT*α *his3*Δ*1 leu2*Δ*0 ura3*Δ*0 lys2*Δ*0 erg24*::*kanMX4*	EUROSCARF; Winzeler *et al.* (1999)
YRS1265	*MATa his3*Δ*1 leu2*Δ*0 lys2*Δ*0 ura3*Δ*0 elo2*::*kanMX4*	EUROSCARF; Winzeler *et al.* (1999)
YRS1116	*MAT*α *ade2 ade3 his3 leu2 ura3 elo3*::*his5 pPS2[URA3 ADE3 ELO3]*	This study
YRS1118	*MAT*α *his3*Δ*200 leu2*Δ*1 ura3-52 elo3*::*his5*	This study
YRS1119	*MAT***a** *his3*Δ*200 leu2*Δ*1 ura3-52 elo3*::*his5*	This study
YRS1247	*MAT***a** *his3*Δ*200 leu2*Δ*1 ura3-52 elo3*::*his5* pPS2[URA3 ADE3 ELO3]	This study
YRS1513	*MAT*α *his3 leu2 ura3 lys2*Δ*0 elo3*::*his5 erg2*::*kanMX4* pPS2[URA3 ADE3 ELO3]	This study
YRS1504	*MAT***a** *his3 leu2 ura3 lys2*Δ*0 elo3*::*his5 erg3*::*kanMX4* pPS2[URA3 ADE3 ELO3]	This study
YRS1510	*MAT*α *his3 leu2 ura3 lys2*Δ*0 elo3*::*his5 erg4*::*kanMX4* pPS2[URA3 ADE3 ELO3]	This study
YRS1506	*MAT*α *his3 leu2 ura3 lys2*Δ*0 elo3*::*his5 erg5*::*kanMX4* pPS2[URA3 ADE3 ELO3]	This study
YRS1508	*MAT*α *his3 leu2 ura3 lys2*Δ*0 elo3*::*his5 erg6*::*kanMX4* pPS2[URA3 ADE3 ELO3]	This study
YRS1514	*MAT*α *his3 leu2 ura3 elo3*::*his5 erg24*::*kanMX4* pPS2[URA3 ADE3 ELO3]	This study
YRS1516	*MAT***a** *his3 leu2 ura3 elo2*::*kanMX4 erg6*::*kanMX4* pRS416-ERG6[URA3 ERG6]	This study
YRS1518	*MAT*α *his3 leu2 ura3 lys2*Δ*0 elo3*::*his5 erg6*::*kanMX4* pRS426-ERG6[URA3 ERG6]	This study
YRS1520	*MAT*α *his3 leu2 ura3 lys2*Δ*0 elo3*::*his5 erg6*::*kanMX4* pME1[LEU2 ERG6]	This study
YRS1519	*MAT*α *his3 leu2 ura3 lys2*Δ*0 elo3*::*his5 erg6*::*kanMX4* pME1$^{ts\#6}$[LEU2 erg6^{ts}]	This study
YRS1550	*MATa his3-*Δ*200 leu2-*Δ*1 ura3-52 trp1 elo3*::*his5 pep4*::*LEU*	This study
YRS1554	*MAT his3 leu2 ura3 elo3*::*his5 end4*::*kanMX4*	This study
YRS1551	*MAT***a** *his3*Δ*1 leu2*Δ*0 met15*Δ*0 ura3*Δ*0 erg6*::*kanMX4* pME1[LEU2 ERG6]	This study

MATERIALS AND METHODS

Strains and Growth Conditions

Yeast strains used in this study are listed in Table 1. Strains bearing single deletions of nonessential *ERG* genes were obtained from EUROSCARF (see www.rz.uni-frankfurt.de/FB/fb16/mikro/euroscarf/index.html; Winzeler *et al.*, 1999). Strains were cultivated at 24, 30, or 37°C in YPD rich media (1% Bacto yeast extract, 2% Bacto peptone [Difco Laboratories Inc., Detroit, MI], 2% glucose) or minimal media. To counterselect for the presence of *URA3* containing plasmids, 5-fluoroorotic acid (5-FOA; bts BioTech Trade and Service Gmbh, St. Leon-Rot, Germany) was added to solid media at 1 g/l. Media supplemented with sterols contained 5 mg/ml Tween 80 and either 20 μg/ml or 10 ng/ml sterols (Sigma Chemical Co., St. Louis, MO). Sterol rescue experiments were performed under anaerobic conditions by placing the plates into an anaerobic jar containing an AnaeroGen sachet (Oxoid Limited, Hampshire, UK). Plates supplemented with brefeldin A contained 50 μg/ml of the drug. For DNA cloning and propagation of plasmids, *E. coli* strain XL1-blue (Stratagene, La Jolla, CA) was used throughout this study.

Plasmid Constructions

To generate the *ADE3*-containing sectoring plasmid used for the synthetic lethal screen, *ELO3* was amplified by PCR using the primer pair ELO3RegF2/ELO3RegR (see Table 2 for sequence of oligonucleotides) and genomic DNA from strain FY1679 as template. The *ELO3* fragment was cloned blunt end into the unique *Sma*I site of pCH1122 to yield pPS2 (Table 3).

The *kanMX4*-containing *ELO3* tester plasmid, pPS5, was generated by cloning the *Not*I/*Sac*I fragment harboring the *kanMX4* gene from pFA6a (Wach *et al.*, 1994) into the corresponding sites of pIBI96 (García-Arranz *et al.*, 1994).

The *ERG6* gene was cloned, after PCR amplification with the primer pair ERG6RegF/ERG6RegR from genomic DNA, as a *Sac*I/*Bam*HI fragment into the corresponding sites of pRS426 (Christianson *et al.*, 1992) to generate pRS426-ERG6. The *ERG6*-containing *Sac*I/*Bam*HI fragment from pRS426-ERG6 was then cloned into the corresponding sites of pRS315 (Sikorski and Hieter, 1989) to generate pME1.

Restriction and ligation of DNA fragments, preparation of plasmid DNA, elution of DNA from low-melt agarose gels and transformation of lithium acetate competent yeast cells was performed according to standard procedures. Enzymes used for DNA manipulations were supplied by MBI Fermentas (St. Leon-Rot, Germany).

Synthetic Lethal Screen

To generate a host strain for the synthetic lethal screen, the *ade2 ade3* parental strain CH1462 was first transformed with pPS2 [*ADE3 URA3 ELO3*] to render it *HIS3*-dependent auxotrophic for histidine (Kranz and Holm, 1990). The *ELO3* gene of this strain was then replaced by the bacterial *his5* gene, amplified with the primer pair ELO3koF/ELO3koR from pFA6a-His3MX6 (Longtine *et al.*, 1998), to generate strain YRS1116. This strain formed red/white colony sectors on YPD and was used for the synthetic lethal screen using a transposon-based knockout library (m-Tn3; see http://ygac.med.yale.edu/; Burns *et al.*, 1994). Approximately 40,000 leucine prototrophic transformants were screened for nonsectoring colonies. Plasmid independence of the nonsectoring phenotype was then assessed by transformation with pPS5. The site of transposon insertion was identified using a vectorette PCR protocol that used the oligonucleotides Bubble-1, -2, and -224, as described (http://genome-www.stanford.edu/group/botlab/protocols/vectorette.html). DNA sequencing was performed on an ABI 373A sequencer using the ABI

Table 2. Primers used in this study

Primer	Sequence
ELO3RegF2	ATCGACGCGTCGACCGAAGTTTTTATTCCGTCCAC
ELO3RegR	ATCCCCCGGGGCACCAAGCCAATAATCTATCA
ERG6RegF	TATGCAGCTCAAAGGTACTACTGTGCTTAATC
ERG6RegR	GATTGAGGATCCTATGGAAACAGTTACGATGC
ELO3koF	ATGAACACTACCACATCTACTGTTATAGCAGCAGTTGCCGACCAGTTCCACGGATCCCCGGGTTAATTAA
ELO3koR	TTAAGCTTTCCTGGAAGAGACCTTGGTGTTAGAGGTCTTGACACCAGTAGGAATTCGAGCTCGTTTAAAC
Bubble-1	GAAGGAGAGGACGCTGTCTGTCGAAGGTAAGGAACGGACGAGAGAAGGGAGAG
Bubble-2	GACTCTCCCTTCTCGAATCGTAACCGTTCGTACGAGAATCGCTGTCCTCTCCTTC
Bubble 224	CGAATCGTAACCGTTCGTACGAGAATCGCT
ERG6mutF	TGAAGAACTGTGGTTTCGAAGTCC
ERG6mutR	AAAATACTGGTCGTTTGCCACG

PRISM BigDye Terminator Cycle Sequencing Ready Reaction Kit with AmpliTaq DNA Polymerase (PE Perkin Elmer-Cetus, Foster City, CA).

Generation of ERG6 *Alleles That Are Temperature Sensitive for Function*

To generate a strain in which the synthetic lethal interaction between *ELO3* and *ERG6* could be conditionally imposed, the 3′ end of *ERG6* was amplified by PCR under error prone conditions (2.5 mM dGTP instead of the normal 250 μM) using the primer pair ERG6mutF/ERG6mutR. The 569-base pair fragment was then cotransformed with *Nhe*I/*Msc*I gapped pME1 into strain YRS1508. One thousand leucine prototrophic colonies were replica plated on 5-FOA media to force loss of pPS2. Uracil auxotrophic colonies were screened for temperature-sensitive growth by replica plating to 37°C. Three plasmids conferring temperature-dependent growth to an *elo3*Δ *erg6*Δ double mutant were isolated and subject to sequence analysis. pME1$^{ts\#6}$ was used for all further studies.

Isolation of Detergent-insoluble Membrane Domains

Detergent-insoluble membrane domains were isolated after floatation on Optiprep gradients (Axis-Shield, Huntingdon, UK) exactly as described by Bagnat *et al.* (2000). Proteins were precipitated with TCA (10%), dissolved in sample buffer, and subjected to SDS-PAGE and Western blot analyses. Raft association of newly synthesized Pma1p was examined as described by Gong and Chang (2001). Lysates of labeled cells (3–4 $OD_{600\ nm}$ equivalents) were extracted with 1% Triton X-100 for 30 min at 4°C. Samples were centrifuged at 100,000 × *g* for 1 h. Pellets were resuspended in 1% SDS. Detergent concentrations in aliquots of total, supernatant, and pellet samples were adjusted for immunoprecipitation.

For lipid analysis, cholesterol was added as internal standard, and lipids were extracted using *n*-heptane. Silylated sterol adducts were then quantified and analyzed by gas chromatography–mass spectroscopy (GC-MS) analysis as described below. Raft association of inositol containing lipids was examined after growing cells in inositol-free media containing 0.1 μCi [^{3}H]*myo*-inositol (Perkin Elmer-Cetus Life Sciences, Cambridge, UK) for 16 h.

Western blot analyses using rabbit anti-Erg6p or anti-Pma1p (1:10,000; G. Daum, Graz University of Technology, Austria) or rabbit anti-Gas1p (1:2000; A. Conzelmann, University of Fribourg, Switzerland) was performed as described before by Schneiter *et al.* (1999).

Protein Secretion and Maturation

Secretion of invertase was assayed as follows. Cells were grown in minimal media containing 5% glucose to an $OD_{600\ nm}$ of 0.2. Invertase expression was induced by resuspending the cells in low glucose media (0.05%), and the cultures were preshifted to 37°C for 15 min. Samples were then removed at the indicated time points, and cells were metabolically poisoned by the addition of 10 mM NaN_3. Invertase activity of equal number of cells was determined as described by Goldstein and Lampen (1975). Carboxypeptidase Y and Gas1p maturation was analyzed as described by Munn *et al.* (1999) and quantified using NHI Image 1.61.

Lipid Analysis

Sterols were isolated as described by Quail and Kelly (1996), using cholesterol as internal standard. GC-MS analysis of silylated sterol adducts was performed on a Hewlett-Packard HP 5890 Series II gas chromatograph (Palo Alto, CA), equipped with a HP 5972 mass selective detector, and HP 5-MS column (cross-linked 5% phenyl methyl siloxane; dimensions: 30 m × 0.25 mm × 0.25 μm film thickness). The following temperature program was run: 1 min at 100°C, 10°C/min to 250°C, and 3°C/min to 300°C. Sterols were identified based on their mass fragmentation pattern and by comparison to commercially available standards.

Inositol-containing lipids were labeled by incubating 10 OD of cells with 30 μCi [^{3}H]*myo*-inositol (Perkin Elmer-Cetus Life Sciences) at either 24 or 37°C for 2 h and analyzed as described by Reggiori *et al.* (1997). For analysis of sphingolipid precursors, 10 OD of cells were incubated with 200 μCi [^{3}H]serine (Perkin Elmer-Cetus Life Sciences) at either 24 or 37°C for 4 h, lipids were extracted with chloroform/methanol (1:1; vol/vol), and mild-base–resistant lipids were analyzed by TLC. Mild-base treatment was performed by incubating lipids in 0.1 M NaOH at 30°C for 1 h.

RESULTS

A Synthetic Lethal Screen with elo3Δ *Identifies Mutations in* ERG6

To investigate the physiological function of very-long-chain fatty acid (C26)-substituted lipids in yeast, we created genetic conditions under which acyl chain elongation from C22/C24 to C26 becomes essential. Therefore, a red/white colony sectoring-based visual screen was performed to identify mutants that are synthetically lethal with mutations in *ELO3*. In an initial evaluation of the screening strategy, a transposon–based knockout library was used to mutagenize the genome (Burns *et al.*, 1994). This approach has the advantage of allowing rapid identification of the mutant loci by a PCR-based protocol (see MATERIALS AND METHODS). Of ~40,000 colonies screened, 19 mutations were isolated that could be grouped into 14 complementation groups.

Table 3. Plasmids used in this study

Designation	Marker(s)	Comments	Source
pRS315	CEN *LEU2*		Sikorski and Hieter (1989)
pRS426	2μm *URA3*		Christianson *et al.* (1992)
pCH1122	CEN *URA3 ADE3*		Kranz and Holm (1990)
mTn3	*LEU2 lacZ*	Transposon-based knock-out library	Burns *et al.* (1994)
pFA6a	kanMX4	*kanMX4* template for gene replacement	Wach *et al.* (1994)
pFA6a-His3MX6	*his5*	*his5* template for gene replacement	Longtine *et al.* (1998)
pIBI96	CEN *LEU2 ELO3*	*ELO3 Kpn*I/*Sal*I genomic fragment in pRS315	García-Arranz *et al.* (1994)
pPS2	CEN *URA3 ADE3 ELO3*	*ELO3* in *Sma*I-site of pCH1122, sectoring plasmid	This study
pPS5	CEN *LEU2 ELO3 kanMX4*	*kanMX4* fragment of pFA6a into *Not*I/*Sac*I of pIBI96	This study
pRS426-ERG6	2μm *URA3*	*ERG6* in *Sac*I/*BamH*I site of pRS426	D. Zweytick and G. Daum, Graz University of Technology
pME1	CEN *LEU2 ERG6*	*ERG6* in *Sac*I/*BamH*I site of pRS315	This study
pME1$^{ts\#6}$	CEN *LEU2 erg6^{ts}*	L341P, temperature-sensitive allele of *ERG6*	This study

One of the mutants isolated in this screen contained a transposon insertion in a gene of the ergosterol biosynthetic pathway, *ERG6* (unpublished data). Erg6p catalyzes the methylation at position 24 of zymosterol to form fecosterol (Gaber *et al.*, 1989). The synthetic lethality of mutations in *ELO3* and *ERG6* was independently confirmed by crossing of the respective single mutants followed by tetrad analysis (unpublished data).

The Interaction between ELO3 *and* ERG6 *Is Specific*

Mutations in *ELO3* and *ELO2/FEN1* have previously been isolated in screens for mutants that are resistant against the immunosupressor SR31747, an inhibitor of the sterol C-8 isomerase, *ERG2* (Silve *et al.*, 1996). In addition, mutations in *ELO2/FEN1* result in resistance against the fungicide fenpropimorph, an inhibitor of the sterol C-14 reductase, encoded by *ERG24* (Ladevèze *et al.*, 1993). These *ELO*-dependent suppressions of inhibitors of the ergosterol biosynthetic pathway, however, have been reported only for the FL100 genetic background, in which both *ERG2* and *ERG24* are essential. In most other genetic backgrounds, *ERG2* and *ERG24* are nonessential (Crowley *et al.*, 1996; Winzeler *et al.*, 1999).

In light of this apparently complex genetic interaction between mutations in *ELO2/3* and the ergosterol biosynthetic pathway, we first determined whether the synthetic lethal interaction that we uncovered between *ELO3* and *ERG6* is specific. Therefore, an *elo3*Δ mutant strain harboring a wild-type *ELO3* gene on an *URA3* marked plasmid (pPS2, strain YRS1247) was crossed to all viable mutants in genes of the ergosterol biosynthetic pathway, i.e., *ERG2*, *ERG3*, *ERG4*, *ERG5*, *ERG6*, and *ERG24*. Viability of the respective double mutant was then assessed by plasmid loss on media containing 5-FOA. As shown in Figure 2A, this analysis revealed that the mutation in *ELO3* is viable with mutations in all the nonessential *ERG* genes, except for *ERG6*, indicating that the synthetic lethal interaction between mutations in *ELO3* and *ERG6* is specific.

To determine whether a mutation in *ERG6* is synthetically lethal with other mutations that affect C26 metabolism, we crossed an *elo2*Δ mutant strain to *erg6*Δ, bearing a wild-type *ERG6* gene on an *URA3*-containing plasmid. Unlike *elo3*Δ mutants, cells defective in *ELO2* are still capable of synthesizing the C26 very-long-chain fatty acid, albeit at reduced efficiency (Oh *et al.*, 1997). Viability of the resulting *elo2*Δ *erg6*Δ double mutant was again assessed by plasmid loss on media containing FOA. As shown in Figure 2B, this analysis revealed that the *elo2*Δ *erg6*Δ double mutant is viable, indicating that the synthetic lethality observed between *ELO3* and *ERG6* is specific for both partners of the respective biosynthetic pathways.

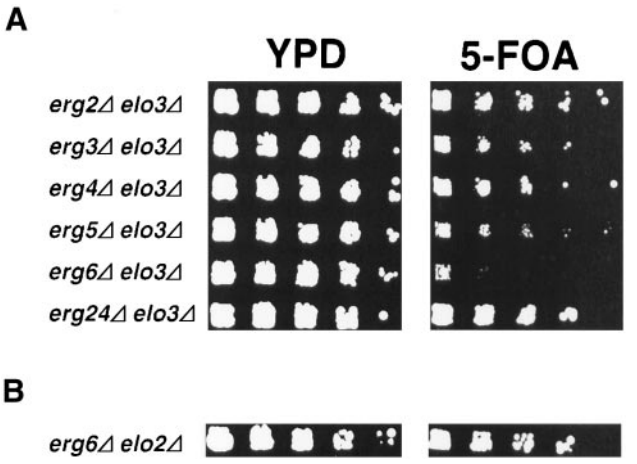

Figure 2. The interaction between *ELO3* and *ERG6* is specific. (A) Growth of the *elo3*Δ mutant (YRS1247) in combination with mutations in genes of the ergosterol biosynthetic pathway—*ERG2* (YRS1513), *ERG3* (YRS1504), *ERG4* (YRS1510), *ERG5* (YRS1506), *ERG6* (YRS1508), and *ERG24* (YRS1514)—was assessed by loss of a plasmid-borne wild-type copy of the *ELO3* gene (pPS2) on media containing 5-FOA. Cells of the indicated genotype were serially diluted 10-fold and replica plated on rich media (YPD) or media containing 5-FOA. Plates were incubated for 3 d at 30°C. (B) *erg6*Δ is viable in combination with mutations in *ELO2*. Viability of an *elo2*Δ *erg6*Δ double mutant (YRS1516) was assessed by loss of a plasmid-borne copy of a wild-type *ERG6* gene (pRS426-ERG6) on media containing 5-FOA.

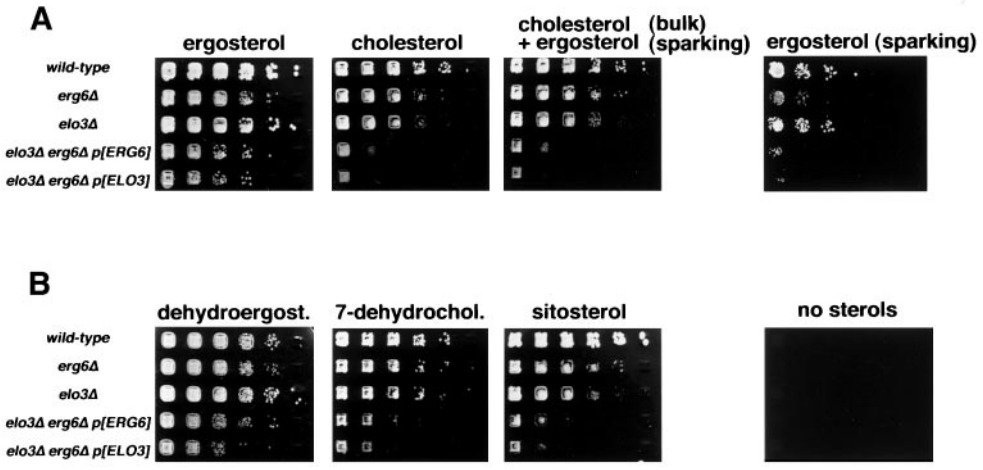

Figure 3. Viability of an *elo3*Δ *erg6*Δ double mutant is rescued by supplementation with ergosterol but not by cholesterol. (A) Viability of the *elo3*Δ *erg6*Δ double mutant was assessed by loss of a plasmid-borne wild-type copy of either the *ERG6* gene (pRS426-ERG6, p[ERG6]) or the *ELO3* gene (pPS2, p[ELO3]) on media containing 5-FOA and supplemented with various sterols. Cells of indicated genotype were serially diluted 10-fold and replica plated on solid media supplemented with the indicated sterols (20 μg/ml), a combination of bulk concentrations of cholesterol (20 μg/ml) and sparking concentrations of ergosterol (10 ng/ml), or sparking concentration of ergosterol only. Plates were incubated under anaerobic conditions for 5 d. (B) Structural requirements of sterols for the rescue of the *elo3*Δ *erg6*Δ double mutant was assessed by plasmid loss on media containing 5-FOA and supplemented with dehydroergosterol (dehydroergost.), 7-dehydrocholestrol (7-dehydrochol.), or sitosterol at bulk concentrations (20 μg/ml), or no sterols.

The Viability of an elo3Δ erg6Δ *Double Mutant Is Rescued by Ergosterol but not by Cholesterol*

Analysis of sterol auxotrophic mutants has revealed distinct cellular functions of sterols that can be fulfilled by supplementations with different concentrations of sterols. The function of sterols required for membrane integrity, termed the bulk function, requires supplementation with 5 μg/ml ergosterol and is also provided by cholesterol. A second function of ergosterol is required for cell cycle progression (Dahl *et al.*, 1987). This sparking function of ergosterol requires 10 ng/ml ergosterol and is not provided by cholesterol but has a stringent structural requirement for ergosterol (Rodriguez and Parks, 1983).

To determine which of these two essential functions of ergosterol is affected in the *elo3*Δ *erg6*Δ double mutant, cells were supplemented with different sterols and grown under anaerobic conditions to allow sterol uptake. Viability of the double mutant was again assessed by monitoring loss of a plasmid-borne copy of a wild-type *ELO3* or *ERG6* gene on media containing 5-FOA. As shown in Figure 3A, the *elo3*Δ *erg6*Δ double mutant was rescued on media supplemented with bulk concentrations of ergosterol. Cholesterol, a mixture containing bulk concentrations of cholesterol and sparking concentrations of ergosterol, or sparking concentrations of ergosterol alone, failed to rescue the double mutant. This observation indicates that the *elo3*Δ *erg6*Δ mutant has a stringent requirement for bulk concentrations of ergosterol that is not provided by cholesterol and that is not depending on sparking concentrations of ergosterol.

To further define the structural requirements for this bulk function-dependent rescue of the *elo3*Δ *erg6*Δ mutant, viability of this strain was assessed on media supplemented with various sterol derivatives. As shown in Figure 3B, growth of the double mutant could also be rescued by supplementation with bulk concentrations of dehydroergosterol (ergosta-5,7,9(11),22-tetraene-3-ol), a sterol with a third double bond in the ring system and a methyl group at position 24 of the aliphatic side chain, as is characteristic for ergosterol. However, dehydrocholestrol (5,7-cholestadien-3-ol), which lacks this methyl group at position 24 but has a double bond configuration of the B ring identical to that of ergosterol, failed to rescue the double mutant, indicating that the presence of the methyl group at position 24, rather than the double-bond configuration of the B ring, is essential for rescue. An ethyl group at position 24, as present in the plant sitosterol, on the other hand, was nonfunctional, because sitosterol did not rescue the double mutant. Taken together, these results indicate that the synthetic lethal interaction between mutations in *ELO3* and *ERG6* is likely to reflect an increased structural requirement for the methyl group at position 24 of the ergosterol molecule in an *elo3*Δ mutant background.

Characterization of a Strain That Is Temperature Sensitive for Erg6p Function

To investigate the increased structural requirement for ergosterol in the *elo3*Δ mutant in more detail, we generated a strain that is temperature sensitive for the function of Erg6p. Therefore, the 3′ end of the *ERG6* gene, covering the carboxy-terminal 120 amino acids, was subject to mutagenesis by error prone PCR (see Figure 4A). After in vivo recombination and plasmid shuffling, three temperature-sensitive *ERG6* alleles were isolated (see MATERIALS AND METHODS). Sequence analysis of one of these alleles revealed a single base substitution in codon 341 (CTA to CCA), resulting in the incorporation of a proline instead of the wild-type leucine at this position of Erg6p.

Analysis of the growth characteristics of this *elo3*Δ *erg6^{ts}* conditional strain revealed that the strain grows like the corresponding wild-type at 24°C but that it rapidly ceases growth upon incubation at nonpermissive conditions (Figure 4B). Plating of cells that have been shifted for up to 8 h to nonpermissive conditions revealed that the capacity of the mutant to restore growth and form colonies when shifted back to permissive conditions (24°C) was not impaired, in-

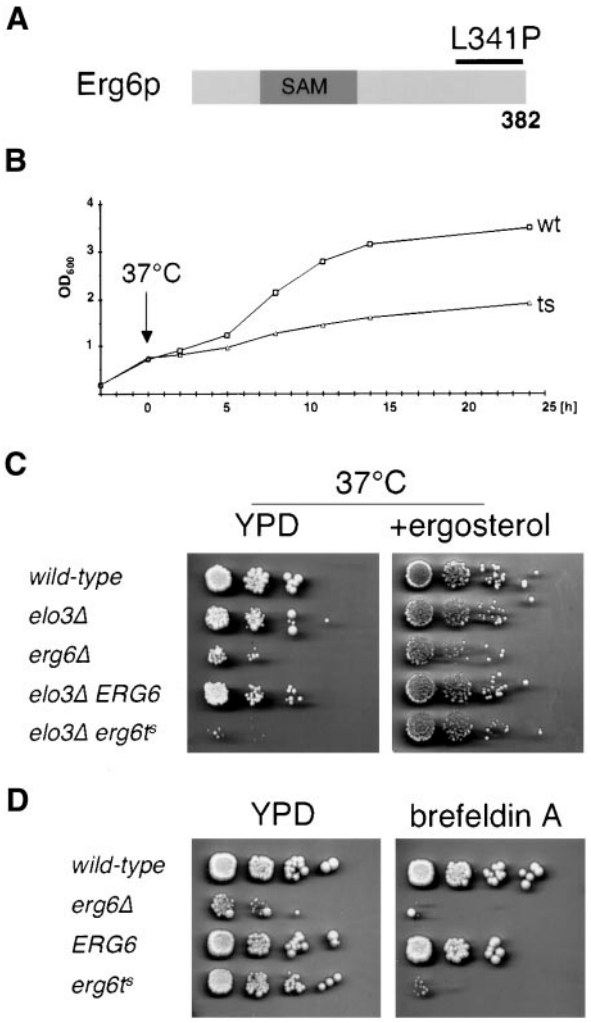

Figure 4. Characterization of an *elo3*Δ *erg6*Δ mutant that is conditionally defective for Erg6p. (A) Structure of the Erg6p protein with the *S*-adenosyl-methionine (SAM)-binding domain indicated. The 3′ end of *ERG6* was subject to mutagenesis using error prone PCR (black bar). The mutant used for further analysis has a leucine to proline substitution at position 341 of Erg6p. (B) Growth of the *elo3*Δ *erg6*^{ts} strain stops at 37°C. The *elo3*Δ *erg6*Δ double mutant containing either a plasmid-borne copy of a wild-type allele of *ERG6* (YRS1520) or containing the *erg6*^{ts} allele (YRS1519), was assessed upon a temperature shift to 37°C by following the optical density in minimal media lacking leucine. (C) Growth of the *elo3*Δ *erg6*^{ts} strain at 37°C is rescued by supplementation with ergosterol. Cells of indicated genotype were serially diluted 10-fold and replica-plated on solid media with ergosterol (+ergosterol) and without (YPD) and incubated at 37°C for 4 d. (D) *erg6*^{ts} is sensitive to brefeldin A. Strains of the indicated genotype were serially diluted 10-fold and replica-plated on media with brefeldin A (+brefeldin A) and without (YPD) and incubated at 24°C for 4 d.

dicating that the metabolic block imposed by the temperature shift was fully reversible. In agreement with these observations, Western blot analysis with an anti-Erg6p antibody revealed that the mutant protein is stable and not subject to temperature-dependent turnover (unpublished data).

The conditional growth phenotype of the *elo3*Δ *erg6*^{ts} mutant could be fully rescued on rich media by ergosterol supplementation, confirming the ergosterol auxotrophic phenotype of the double mutant that was so far based on plasmid loss on 5-FOA containing synthetic media (Figure 4C). Analysis of the in vivo activity of the temperature-sensitive enzyme by labeling cells with [^{3}H]methionine revealed an ~800-fold reduced activity of the enzyme at permissive conditions. This activity declined to undetectable levels upon incubation of cells at nonpermissive conditions (unpublished data). Consistent with this low activity of the conditional Erg6p allele, *erg6*Δ mutant cells bearing this allele are sensitive to brefeldin A, as is an *erg6*Δ null allele (Shah and Klausner, 1993; Figure 4D).

Characterization of the Secretory Pathway in the elo3Δ erg6^{ts} *Conditional Mutant*

To determine whether protein maturation and secretion were conditionally affected in the *elo3*Δ *erg6*^{ts} mutant strain, the kinetics of invertase induction and secretion was analyzed (Novick and Schekman, 1979). Induction and secretion of invertase in the *elo3*Δ *erg6*^{ts} conditional mutant was comparable to that observed in the *elo3*Δ *ERG6* strain, indicating that vesicular transport from the ER to the plasma membrane is not affected by the inactivation of Erg6p in the *elo3*Δ mutant background (Figure 5A).

To examine whether vesicular transport between the Golgi apparatus and the vacuole was affected, transport of the soluble vacuolar hydrolase carboxypeptidase Y (CPY) was examined by pulse-chase analysis. CPY leaves the ER as a 67-kDa preprotein to mature in the Golgi apparatus to a 69-kDa form, which is cleaved to the active 61-kDa protease in the vacuole. After a preshift to 37°C for 15 min, the *elo3*Δ *erg6*^{ts} mutant exhibited wild-type kinetics of CPY maturation, indicating that vesicular transport between ER and the vacuole was not impaired by inactivation of Erg6p in an *elo3*Δ mutant background (Figure 5B).

To complete the analysis of the secretory pathway, we examined whether maturation of the GPI-anchored membrane protein Gas1p was affected. Gas1p exits the ER as a 105-kDa precursor and matures in the Golgi apparatus to a 125-kDa form (Fankhauser and Conzelmann, 1991). The accumulation of the ER form of Gas1p is a sensitive assay to detect perturbations in ER-to-Golgi transport. Western blot analysis revealed wild-type maturation of Gas1p in *erg6*Δ but a strong accumulation of the ER precursor of Gas1p in the *elo3*Δ *erg6*^{ts} mutant strain, irrespective of whether the mutant was incubated at permissive or nonpermissive conditions (unpublished data). Accumulation of the ER form of Gas1p was also observed in the *elo3*Δ mutant alone and in the *elo3*Δ *erg6*Δ double mutant bearing a wild-type copy of *ERG6* on a plasmid. To determine whether there is a superimposed delay in Gas1p maturation by the inactivation of Erg6p in an *ELO3* mutant background, we followed maturation of Gas1p by pulse-chase analysis and immunoprecipitation. This analysis failed to reveal a significant delay in Gas1p maturation by the reduction of Erg6p activity in the *elo3*Δ mutant background (Figure 5C). Taken together, these results indicate that the efficiency of the secretory pathway is not generally perturbed in the *elo3*Δ *erg6*^{ts} conditional strain.

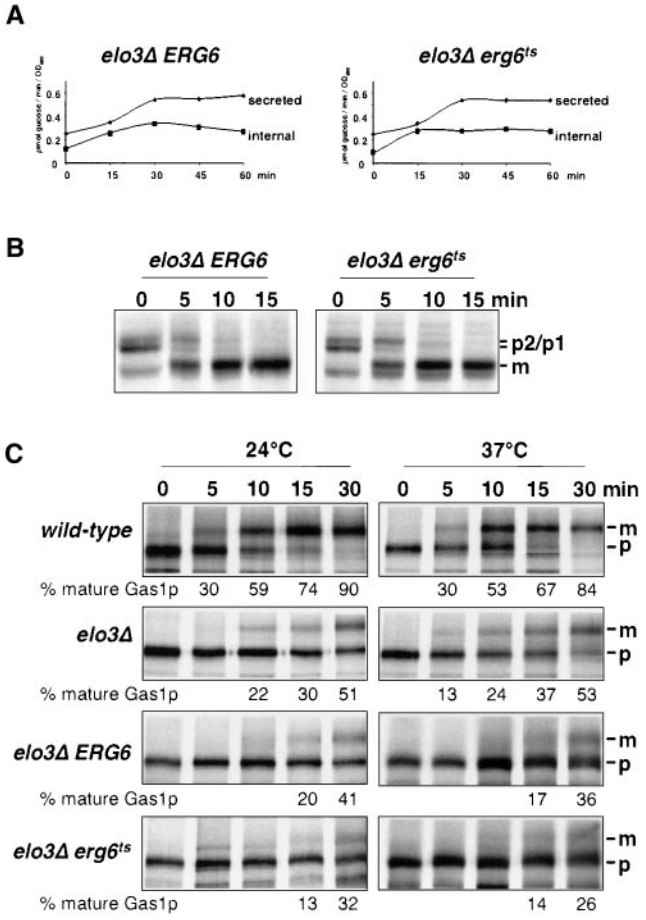

Figure 5. Characterization of the secretory pathway in the *elo3*Δ *erg6*^{ts} mutant. (A) Secretion of invertase was analyzed in the *elo3*Δ *erg6*Δ double mutant strain bearing a plasmid-borne copy of either *ERG6* (*elo3*Δ *ERG6*, YRS1520) or *erg6*^{ts} (*elo3*Δ *erg6*^{ts}, YRS1519). Cells were preshifted to 37°C for 15 min before invertase induction by glucose limitation. Samples were removed at the time points indicated and the activity of internal and secreted invertase was determined. (B) Maturation of CPY was analyzed in the *elo3*Δ *erg6*Δ double mutant strain bearing a plasmid-borne copy of either *ERG6* (*elo3*Δ *ERG6*, YRS1520) or *erg6*^{ts} (*elo3*Δ *erg6*^{ts}, YRS1519). Cells were preshifted to 37°C for 15 min before labeling with [^{35}S]methionine for 5 min and chasing for the time indicated. CPY was recovered by immunoprecipitation, subjected to SDS-PAGE, and visualized by autoradiography. The position of precursor (p1, ER; p2, Golgi) and mature CPY (m, vacuolar) is indicated. (C) Maturation of Gas1p was analyzed in wild-type (FY1679a), *elo3*Δ (YRS1118), and the *elo3*Δ *erg6*Δ double mutant strain bearing a plasmid-borne copy of either *ERG6* (*elo3*Δ *ERG6*, YRS1520) or *erg6*^{ts} (*elo3*Δ *erg6*^{ts}, YRS1519). Cells were incubated at 24°C or preshifted to 37°C for 15 min before pulse-chase analysis and immunoprecipitation. The positions of ER precursor (p, 105 kDa) and mature Gas1p (m, 125 kDa) are indicated. Quantification of the degree of Gas1p maturation is shown below.

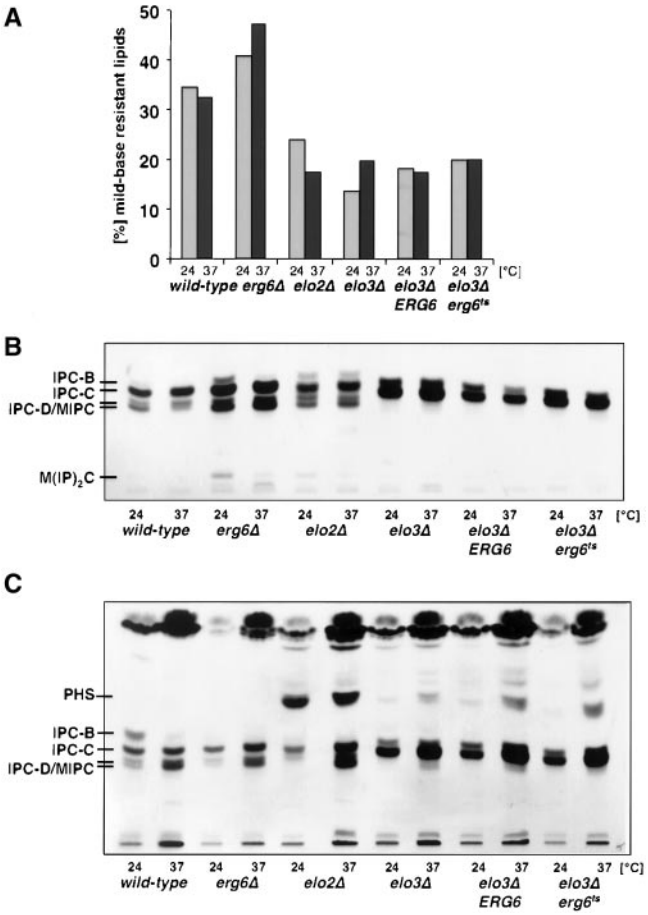

Figure 6. elo3Δ erg6^{ts} has a sphingolipid composition characteristic for *elo3*Δ. (A) Sphingolipid synthesis in wild-type (FY1679a), *erg6*Δ (YRS1266), *elo2*Δ (YRS1265), *elo3*Δ (YRS1118), and the *elo3*Δ *erg6*Δ double mutant strain bearing a plasmid-borne copy of either *ERG6* (*elo3*Δ *ERG6*, YRS1520) or *erg6*^{ts} (*elo3*Δ *erg6*^{ts}, YRS1519) was assessed by labeling cells at either 24 or 37°C with [^{3}H]inositol for 2 h. Lipids were extracted, and label incorporated into the mild-base–resistant sphingolipid fraction was determined in comparison to label incorporated into the total lipid fraction. (B) Sphingolipid composition in strains of indicated genotype was analyzed by TLC and fluorography. Cells were labeled at either 24 or 37°C with [^{3}H]inositol for 2 h, and mild-base–resistant lipids were separated by TLC. The position of different sphingolipid species is indicated to the left. MIPC, mannosyl-inositolphosphorylceramide; $M(IP)_2C$, mannosyl-diinositolphosphorylceramide. (C) Comparison of the levels of sphingolipid precursors in strains of indicated genotype. Cells were labeled at either 24 or 37°C with [^{3}H]serine for 4 h, and mild-base–resistant lipids were separated by TLC. The position of sphingolipid precursors and mature sphingolipid species is indicated to the left. MIPC, mannosyl- inositolphosphorylceramide.

The elo3Δ erg6^{ts} *Mutant Has a Sphingolipid Composition Characteristic of* elo3Δ

To determine whether inactivation of Erg6p affects sphingolipid synthesis in the double mutant, cells were preshifted to nonpermissive conditions and incorporation of [^{3}H]inositol into the mild-base–resistant lipid fraction was examined. This analysis revealed an approximately twofold decrease in the incorporation of [^{3}H]inositol into sphingolipids in cells mutant for either *ELO2* or *ELO3*, irrespective of the activity of Erg6p (Figure 6A). Inactivation of *ERG6* alone, however, resulted in a slight increased incorporation of label into sphingolipids.

TLC analysis of the sphingolipid classes synthesized under these conditions revealed a predominance of IPC-C (inositolphosphorylceramide-C) species at the expense of the more complex mannosylated sphingolipids in all strains with mutations in *ELO3*, irrespective of Erg6p activity (Figure 6B). These alterations in sphingolipid levels and composition in the *elo3*Δ mutant are in agreement with previous analyses (Oh *et al.*, 1997; David *et al.*, 1998). The IPC-C species produced in an *elo3*Δ mutant background has a somewhat lower mobility compared with the IPC-C species of wild-type cells, consistent with the idea that this sphingolipid is less hydrophobic because of the presence of a shorter acyl chain. Taken together, the results of the sphingolipid analysis indicate that sphingolipid synthesis/composition of the *elo3*Δ mutant is not affected by the activity of Erg6p.

The sphingolipid precursors, ceramide and phytosphingosine (PHS), regulate cell growth by activation of different signaling pathways (Hannun and Luberto, 2000). To determine whether accumulation of these signaling lipids results in growth arrest of the *elo3*Δ *erg6^{ts}* conditional mutant, ceramide and PHS levels were examined by labeling cells with [^{3}H]serine (Figure 6C). This analysis revealed a strong accumulation of PHS in the *elo2*Δ mutant strain and lower levels of PHS in all strains with mutations in *ELO3*, irrespective of Erg6p activity. These results thus indicate that the activity of Erg6p does not affect sphingolipid signaling in an *elo3*Δ mutant background.

The elo3Δ erg6^{ts} *Mutant Affects Raft Association of the Plasma Membrane ATPase*

Given that sphingolipid synthesis is continuing in the conditional mutant under nonpermissive conditions, we wondered whether membrane raft formation might be impaired. Therefore, raft association of two marker proteins, the GPI-anchored Gas1p, and the plasma membrane ATPase, Pma1p, was investigated (Bagnat *et al.*, 2000). After two successive rounds of extraction with the nonionic detergent Triton X-100 and floatation in density gradients, both marker proteins were recovered in the detergent-insoluble fraction of the gradient when membranes of cells that were cultivated at permissive conditions were analyzed. On incubation of the conditional *elo3*Δ *erg6^{ts}* mutant at nonpermissive conditions for 2 h, however, raft association of Pma1p but not that of Gas1p was specifically impaired (Figure 7). It is important to note that unambiguous determination of raft association of Pma1p in the mutant required analysis by two successive gradients as the portion of Pma1p from the detergent-resistant fraction of the first gradient was recovered in the detergent-soluble fraction of the second gradient. Raft association of Pma1p was not impaired in the *elo3*Δ *erg6*Δ double mutant harboring a plasmid-borne wild-type copy of *ERG6,* indicating that steady state raft association of Pma1p is dependent on Erg6p activity in an *elo3*Δ mutant background.

To examine whether raft association of Pma1p is detergent induced, an equal number of cells of the two genotypes that had been incubated at nonpermissive conditions for 2 h was mixed, and raft association of Gas1p and Pma1p was reexamined. This analysis revealed that Gas1p maintained its raft association, but Pma1p was now observed in both the detergent-resistant and the -soluble fractions of the gradient.

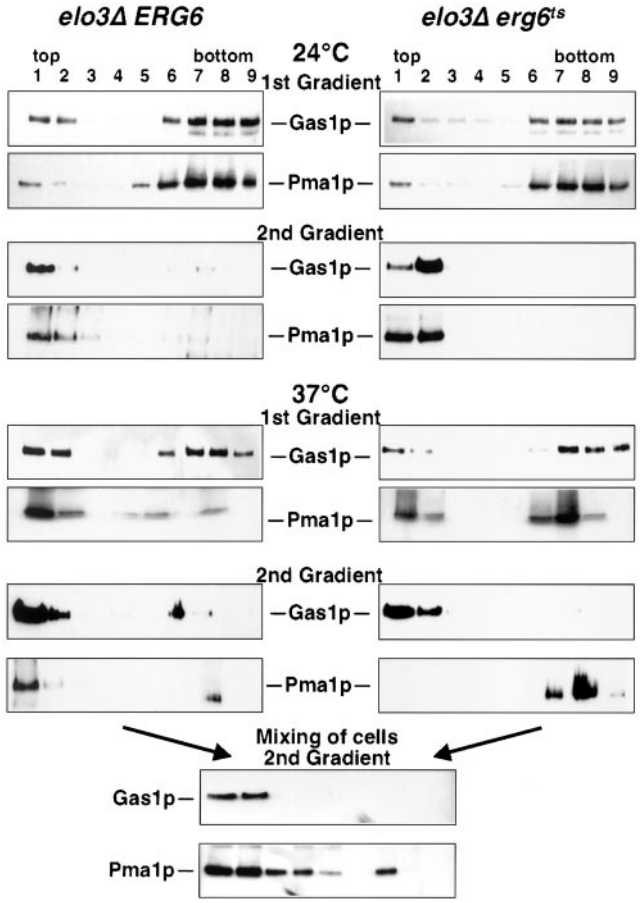

Figure 7. elo3Δ erg6^{ts} affects steady state raft association of the plasma membrane ATPase. Raft association of Gas1p and the plasma membrane ATPase, Pma1p, in the *elo3*Δ *erg6*Δ double mutant strain bearing a plasmid-borne copy of either *ERG6* (*elo3*Δ *ERG6*, YRS1520) or *erg6^{ts}* (*elo3*Δ *erg6^{ts}*, YRS1519). Cells were cultivated at 24°C or shifted to nonpermissive conditions (37°C) for 2 h, before isolation of detergent-resistant membranes by either one (1st Gradient) or two rounds (2nd Gradient) of detergent extraction and floatation on density gradients (Bagnat *et al.*, 2000). The position of mature Gas1p and that of Pma1p is indicated. For the mixing experiment, cells of the two genotypes were mixed at a 1:1 ratio after incubation at nonpermissive conditions for 2 h, and detergent solubility of Gas1p and Pma1p was assessed after two successive rounds of detergent extraction and floatation on density gradients. All blots were processed under comparable conditions.

elo3Δ *Conditionally Affects Stability of the ATPase at the Plasma Membrane*

Pma1p has recently been shown to move into raft domains during biosynthetic transport to the plasma membrane (Bagnat *et al.*, 2001; Gong and Chang, 2001; Ferreira *et al.*, 2002; Lee *et al.*, 2002). Raft association of Pma1p is required for proper delivery to the plasma membrane because inhibition of raft association results in rerouting of the protein to the vacuole where it becomes degraded (Bagnat *et al.*, 2001). To examine whether raft association required for biosynthetic transport of Pma1p to the plasma membrane is affected by inactivation of Erg6p in an *elo3*Δ mutant background, cells

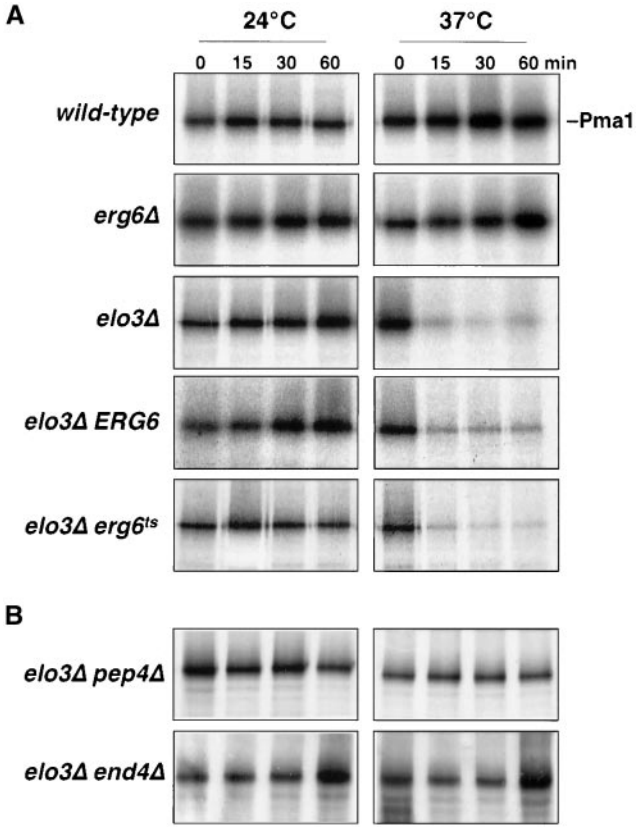

Figure 8. *elo3*Δ affects the stability of newly synthesized Pma1p. (A) The half-life of newly synthesized Pma1p in wild-type (FY1679a), *elo3*Δ (YRS1118), and *erg6*Δ (YRS1266), and the *elo3*Δ *erg6*Δ double mutant strain bearing a plasmid-borne copy of either *ERG6* (*elo3*Δ *ERG6*, YRS1520) or *erg6*^{ts} (*elo3*Δ *erg6*^{ts}, YRS1519) was assessed by pulse-chase analysis and immunoprecipitation. Cells were cultivated at 24°C or preshifted to 37°C for 15 min before labeling under the conditions indicated. (B) Pma1p degradation in the *elo3*Δ mutant requires *PEP4* and *END4*. Turnover of newly synthesized Pma1p in *elo3*Δ *pep4*Δ (YRS1550) and *elo3*Δ *end4*Δ (YRS1554) double mutant strains was assessed as in A.

were pulse-labeled and maturation of Pma1p was followed by immunoprecipitation. This analysis revealed rapid turnover of Pma1p in the *elo3*Δ mutant when cells were incubated at 37°C (Figure 8A). Under these conditions, 80% of newly synthesized Pma1p was rapidly degraded, irrespective of the activity of Erg6p. These results thus indicate that mutations in *ELO3* affect raft association of newly synthesized Pma1p at 37°C.

The increased turnover of newly synthesized Pma1p in the *elo3*Δ mutant occurs by vacuolar degradation because Pma1p is stabilized by a mutation in the vacuolar hydrolase Pep4p (Jones, 1991). Moreover, transport of Pma1p to the vacuole appears to occur after it has reached the plasma membrane, because it is stabilized by blocking internalization from the cell surface in *end4*Δ cells (Raths *et al*., 1993; Figure 8B). Thus, Elo3p is required for stabilizing newly synthesized Pma1p at the plasma membrane at 37°C.

To examine at which point along the secretory pathway raft association of Pma1p is affected in *elo3*Δ, the detergent

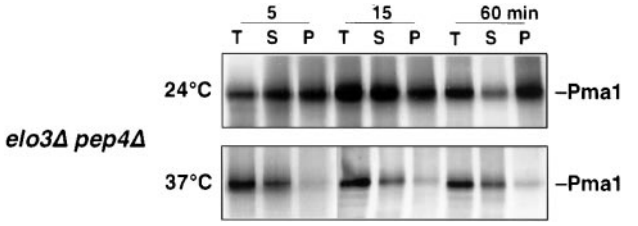

Figure 9. Newly synthesized Pma1p does not acquire detergent resistance in *elo3*Δ at 37°C. *elo3*Δ *pep4*Δ (YRS1550) cells were incubated at the indicated temperatures for 15 min, pulse-labeled for 5 min, and chased for 15 and 60 min. Cell lysates (T) were then extracted with Triton X-100 and separated into a soluble (S) and insoluble (P) fractions. Pma1p was immunoprecipitated and analyzed by SDS-PAGE and fluorography.

solubility of Pma1p was assessed by pulse labeling. To stabilize newly synthesized Pma1p, this analysis was performed in an *elo3*Δ *pep4*Δ double mutant strain. As shown in Figure 9, Pma1p becomes detergent insoluble already after 5 min in cells cultivated at 24°C. At 37°C, however, Pma1p does not acquire detergent resistance in *elo3*Δ, indicating that *elo3*Δ affects raft association of Pma1p early in its biosynthetic transport and that raft association of Pma1p is important for maintaining its stability at the plasma membrane.

ERG6 *Is Required for Maintaining Raft Domains in* elo3Δ

Given the observation that the conditional *elo3*Δ *erg6*^{ts} mutant affects steady state raft association of Pma1p but not Gas1p, we examined whether lipid rafts by themselves were affected. Therefore, the sterol content of the detergent-resistant membrane fraction of mutant cells grown at permissive conditions or incubated at nonpermissive conditions for 2 h was determined by quantitative GC-MS. This analysis revealed that 30% of free sterols were raft associated in an *elo3*Δ *ERG6* control strain at either 24 or 37°C. In the *elo3*Δ *erg6*^{ts} conditional mutant, however, the content of raft-associated sterols was reduced threefold at permissive conditions and further declined more than sixfold upon incubation at nonpermissive conditions (Figure 10A). These results thus indicate that preexisting raft structures are affected upon inactivation of Erg6p in an *elo3*Δ mutant strain.

To determine whether the decrease in raft lipids observed in the conditional mutant is specific for sterols, we examined the sphingolipid content of raft membranes in the two strains. Therefore, cells were labeled with [^{3}H]*myo*-inositol for 16 h and raft association of mild-base–resistant lipids was determined. This analysis revealed an approximately twofold elevated level of sphingolipids in the detergent-resistant membrane fraction of the conditional mutant (Figure 10B). Unlike the sterol content, however, the sphingolipid content of raft membranes did not decline upon incubation of these cells at nonpermissive conditions. These results thus indicate that the aberrant sterols in raft membranes of the conditional mutant do not resist detergent extraction.

A quantitative analysis of total cellular sterols revealed significantly higher sterol levels in the *elo3*Δ and *erg6*Δ single

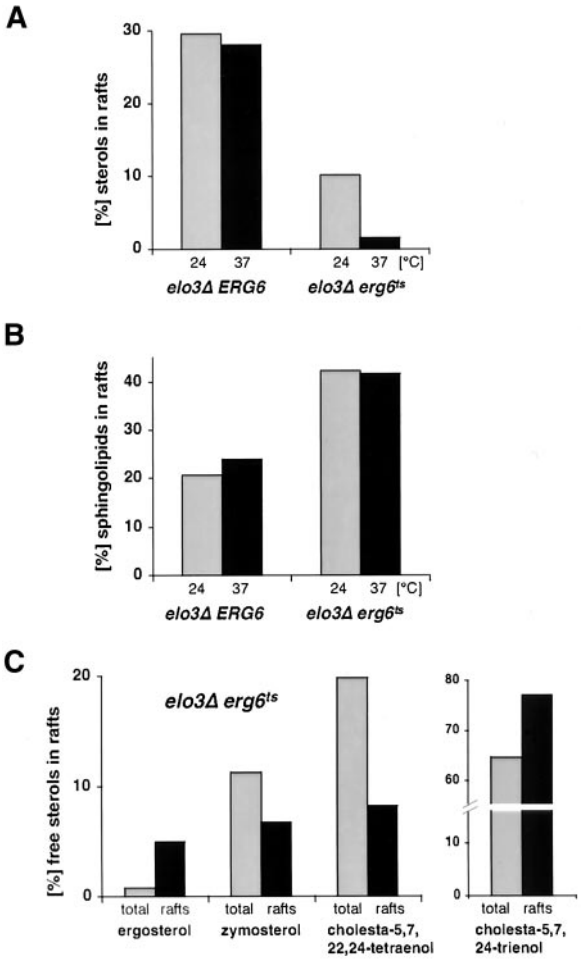

Figure 10. The *elo3*Δ *erg6*^{ts} conditional mutant affects membrane raft domains. (A) Comparison of free sterol levels in detergent-resistant membrane domains from the *elo3*Δ *erg6*Δ double mutant strain bearing a plasmid-borne copy of either *ERG6* (*elo3*Δ *ERG6*, YRS1520) or *erg6*^{ts} (*elo3*Δ *erg6*^{ts}, YRS1519), cultivated at permissive conditions (24°C) or shifted to nonpermissive conditions (37°C) for 2 h. Total membranes and detergent-resistant membrane domains were isolated by two successive rounds of detergent extraction and floatation in density gradients. Sterols present in total and detergent-resistant membranes were quantified by comparison to an internal standard by GC-MS analysis, and the proportion of sterols present in the detergent-resistant membrane fraction relative to the amount of sterols in total membranes is shown. (B) Comparison of sphingolipid levels in the detergent-resistant membrane fraction from the *elo3*Δ *erg6*Δ double mutant strain bearing a plasmid-borne copy of either *ERG6* (*elo3*Δ *ERG6*, YRS1520) or *erg6*^{ts} (*elo3*Δ *erg6*^{ts}, YRS1519), cultivated at permissive conditions (24°C) or shifted to nonpermissive conditions (37°C) for 2 h. Cells were labeled with [^{3}H]*myo*-inositol for 16 h. Total and detergent treated membranes were isolated by floatation in density gradients. Sphingolipids were quantified after mild-base treatment of lipid extracts. The proportion of mild-base–resistant lipids present in the detergent-resistant membrane fraction relative to that of total membranes is shown. (C) Comparison of the free sterol composition of total membranes (total) and the detergent-insoluble membrane fraction (rafts) of the *elo3*Δ *erg6*^{ts} (YRS1519) conditional mutant at permissive conditions. Total and detergent-resistant membrane domains were isolated by two successive rounds of flotation in density gradients. The sterol composition of the two membranes was analyzed by GC-MS and the proportion of different sterols present in the two membranes is shown.

mutants. Combining the two mutations results in a further increase in total sterol levels, resulting in four times elevated total saponifiable sterol levels (Table 4). A compositional analysis of the total saponifiable sterols in the conditional mutant revealed a sterol pattern characteristic of an *erg6*Δ single mutant with zymosterol (45.4%) and cholesta-5,7,24-trienol (33.7%) as the major sterols, which is in agreement with a previous analysis of the sterol composition of an *erg6*Δ mutant (Munn *et al.*, 1999; Table 5). The low ergosterol content observed in the conditional mutant indicates that the temperature-sensitive allele of *ERG6* has a greatly reduced activity already at the permissive temperature and that the plasmid-borne wild-type copy of *ERG6* also does not fully complement the *erg6*Δ deletion.

Given the fact that the conditional mutant strain has a fourfold increased level of total sterols but a threefold reduced level of sterols in detergent-resistant membranes, we examined whether detergent-insoluble membrane domains exhibit preference for certain sterol species. Therefore, the composition of free (nonesterified) sterols in the detergent-insoluble membrane fraction from an *elo3*Δ *erg6*^{ts} conditional strain cultivated at permissive conditions was examined by GC-MS. This analysis revealed a sevenfold enrichment of ergosterol in the detergent-resistant membrane fraction (Figure 10C). Zymosterol and cholesta-5,7,22,24-tetraenol, on the other hand, are deenriched in the raft fraction. Given that ergosterol accounts for only ~1.3% of the total saponifiable sterols in an *elo3*Δ *erg6*^{ts} conditional mutant (Table 5) in which 10% of the sterols are raft associated, a sevenfold enrichment of ergosterol in these raft structures, suggests that ergosterol synthesis and hence Erg6p activity becomes limiting for the maintenance of raft domains in this strain.

To determine whether the observed preference of membrane rafts for ergosterol is specific for *elo3*Δ mutant cells or a more general property of yeast membranes, the sterol composition of membrane rafts of cells making normal C26-substituted sphingolipids was analyzed. Therefore, the sterol composition of total and detergent-resistant membranes from an *erg6*Δ mutant that harbors a plasmid-borne wild-type allele of *ERG6* was analyzed by quantitative GC-MS. This analysis revealed that both ergosterol and cholesta-5,7,24-trienol were slightly enriched in raft membranes, whereas zymosterol and other low abundant sterols such as fecosterol and 14-desmethyl-lanosterol were deenriched to undetectable levels (Figure 11). These data are consistent with the proposal that ergosterol is preferentially included in raft membranes in cells that have normal C26-substituted sphingolipids. However, given that *erg6*Δ mutants are viable in an *ELO3* wild-type background, this preference is much less stringent.

DISCUSSION

We report a specific genetic interaction between mutations in genes required for fungal specific lipid modifications: one in the synthesis of long-chain fatty acids and the other in the synthesis of sterols. The synthetic lethality between mutations in *ELO3* and *ERG6* is likely due to a vital interaction of the respective lipid products, because the viability of the double mutant is rescued by supplementation with ergosterol. The fact that the double mutant is only rescued by sterols that have a methyl group at position 24 of the side

Table 4. Total sterol content of mutant strains at 24°C

	Wild-type	*elo2*Δ	*elo3*Δ	*erg6*Δ	*elo3*Δ *ERG6*	*elo3*Δ *erg6^{ts}*
μg sterol/OD	1.17 ± 0.13	1.19 ± 0.09	1.71 ± 0.19	2.46 ± 0.05	2.61 ± 0.24	3.73 ± 0.40

chain indicates that the *elo3*Δ mutant has a stringent structural requirement for this otherwise nonessential sterol modification.

Cross-talk between Lipid Biosynthetic Pathways

Comparison of the lipid composition of *erg6*Δ, *elo3*Δ, and double mutant strains revealed apparently compensatory changes in sterol and sphingolipid synthesis, indicating that the two lipid biosynthetic pathways must be under coordinate control (Swain *et al.*, 2002). First, the *erg6*Δ mutant displayed an increased rate of incorporation of radiolabeled inositol into mild-base–resistant lipids and a ~2.1-fold increase in total sterol levels, suggesting that the absence of ergosterol in this strain is compensated by an increase in both sterol and sphingolipid levels (Figure 6A, Table 4). Second, mutations in *ELO3* result in a reduced rate of sphingolipid synthesis and in the absence of the more complex mannosylated sphingolipid species. These changes in the sphingolipid pattern of an *elo3*Δ mutant appear to be compensated by a ~1.5-fold increase in sterol levels. The sterol composition of the *elo3*Δ mutant, however, is comparable to that of wild-type cells, indicating that the altered sphingolipid composition affects sterol levels only but not the activity of individual sterol biosynthetic enzymes. Third, the combination of mutations in both *ELO3* and *ERG6* does not further affect sphingolipid synthesis, but results in an additional increase in total sterol levels, and a sterol composition characteristic of an *erg6*Δ mutant.

Raft Formation in the elo3Δ erg6Δ *Double Mutant*

A common structural function of sphingolipids and sterols is their association into membrane microdomains/rafts. Formation of these raft domains is important for lateral sorting of proteins and for signal transduction (Brown and Rose, 1992; Simons and Ikonen, 1997). Previous studies have established that depletion of either sterols or sphingolipids in yeast affects raft association of Gas1p and Pma1p (Bagnat *et al.*, 2000, 2001; Lee *et al.*, 2002). In our strains, sterols and sphingolipids are not depleted, but their structure and composition is altered. This affects raft association of the two marker proteins differently. Although the GPI-anchored Gas1p remains raft associated in the *elo3*Δ *erg6^{ts}* conditional strain, Pma1p becomes detergent soluble. Analysis of the composition of the detergent-resistant lipids in this strain revealed that the sterol content is greatly reduced, whereas the sphingolipid content of raft membranes is increased, suggesting that sphingolipids compensate for the absence of appropriate sterols to maintain raft function in this strain, at least at 24°C. Under more stringent conditions (37°C), the stability of preexisting raft domains becomes impaired to a point where they can no longer resist detergent solubilization, resulting in the release of Pma1p but not Gas1p. The observation that Gas1p maintains detergent resistance may indicate that under these conditions this GPI-anchored protein partitions into a domain that has a different lipid composition than the typical raft, i.e., a sphingolipid-rich but ergosterol-poor domain.

Analysis of the sterol composition of the raft membranes in the conditional strain revealed a strong enrichment in ergosterol. This observation and the fact that the *elo3*Δ *erg6*Δ double mutant can only be rescued by sterols that have a methyl group in the aliphatic side chain suggests that C24-substituted sphingolipids have an increased structural requirement for this methyl group. This notion is supported by a recent biophysical study, which demonstrates that ergosterol is significantly more strongly domain-promoting than cholesterol (Xu *et al.*, 2001). Moreover, in *erg6*Δ mutants the GPI-anchored plasma membrane protease, Yps1p, is mistargeted to the vacuole, indicating that the precise structure of the sterol is important for raft function in vivo (Sievi *et al.*, 2001).

Raft Formation in the elo3Δ *Mutant*

Stable delivery of Pma1p to the plasma membrane requires functional rafts (Bagnat *et al.*, 2001; Gong and Chang, 2001;

Table 5. Total sterol composition of mutant strains at 24°C

	Wild-type	*elo2*Δ	*elo3*Δ	*erg6*Δ	*elo3*Δ *ERG6*	*elo3*Δ *erg6^{ts}*
Zymosterol	9.8 ± 1.3	14.6 ± 1.2	15.3 ± 1.8	35.4 ± 1.5	18.1 ± 2.5	45.4 ± 1.9
Fecosterol	9.3 ± 1.3	8.8 ± 0.4	14.1 ± 1.0	n.d.	14.4 ± 0.9	n.d.
Cholesta-5,7,24-trienol	n.d.	n.d.	n.d.	42.1 ± 2.5	10.1 ± 2.5	33.7 ± 2.6
Cholesta-5,7,22,24-tetraenol	n.d.	n.d.	n.d.	10.2 ± 0.1	2.0 ± 0.3	10.4 ± 0.6
Ergosterol	70.6 ± 1.4	63.4 ± 3.0	58.2 ± 2.9	n.d.	37.5 ± 2.3	1.3 ± 0.3
Others	8.7 ± 5.0	9.8 ± 3.4	7.9 ± 1.4	9.5 ± 1.0	12.2 ± 3.5	2.0 ± 0.6

n.d.; not detectable. Values are % of total. Other sterols are lanosterol, 14-desmethyl-lanosterol, 4-methyl-zymosterol, cholesta-5,8,24-trienol, episterol, cholesta-7,24-dienol, and ergosta-5,7-dienol.

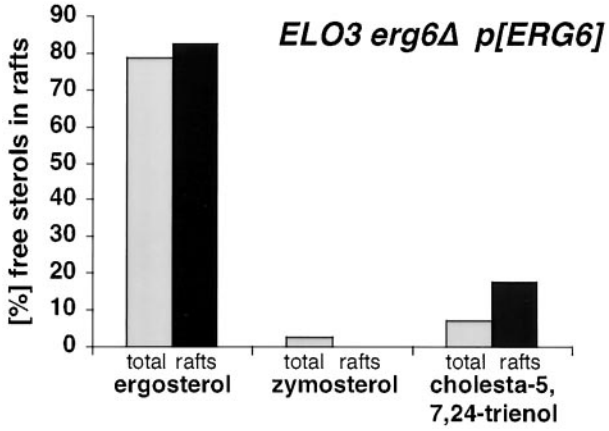

Figure 11. Sterol composition in raft domains of *ELO3* cells. Comparison of the free sterol composition of total membranes (total) and the detergent-insoluble membrane fraction (rafts) in cells that have C26 substituted sphingolipids, but a mixture of different sterols (*ELO3 erg6*Δ p[ERG6]; YRS1551). Detergent-resistant membrane domains were isolated by two successive rounds of detergent extraction followed by flotation in density gradients. Sterol composition was analyzed by GC-MS.

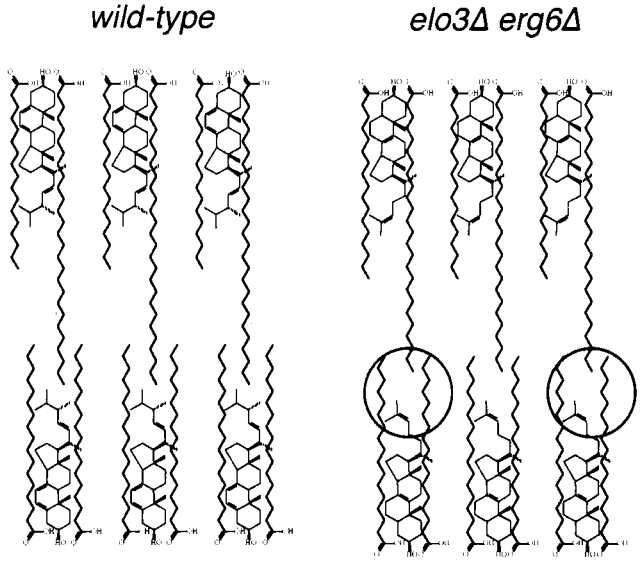

Figure 12. Comparison of the structure of the plasma membrane of wild-type and *elo3*Δ *erg6*Δ mutant cells. Schematic model of the presumed structure of the hydrophobic core of the plasma membrane of wild-type cells compared with cells that contain C22-substituted sphingolipids and zymosterol instead of ergosterol. Alteration in the hydrophobic core of the mutant membrane is encircled. See text for details.

Lee *et al.*, 2002). The observation that ~80% of newly synthesized Pma1p are rapidly turned over in the *elo3*Δ mutant at 37°C through internalization from the cell surface and delivery to the vacuole, indicates that nonraft-associated Pma1p is unstable when it reaches the plasma membrane. A similar phenotype, raft-dependent stabilization of surface delivered Pma1p has been observed with a mutant allele of Pma1p, Pma1–10 (Gong and Chang, 2001). In this case, raft association of Pma1–10 was suggested to be required but not sufficient for its subsequent stabilization at the cell surface. This is consistent with observations made with a second allele of Pma1, Pma1-G381A, which remains raft associated but nevertheless fails to become stabilized at the cell surface (Ferreira *et al.*, 2002).

Pma1p that has entered rafts and that has been delivered to the plasma membrane in *elo3*Δ at 24°C, however, remains stable even if raft function is subsequently impaired by shifting cells to 37°C, as indicated by the observation that steady state raft association of Pma1p is not affected in the *elo3*Δ *ERG6* mutant at 37°C. These observations may indicate that *elo3*Δ at 37°C affects raft assembly but that preexisting structures remain stable unless ergosterol is depleted.

*elo3*Δ mutants display a number of lipid alterations that potentially could affect raft formation, particularly when combined with mutations in the sterol biosynthetic pathway. First, *elo3*Δ mutant cells have reduced levels of sphingolipids. A complete block in sphingolipid synthesis as achieved using a conditional allele of serine palmitoyltransferase (*lcb1–100*; Sütterlin *et al.*, 1997), which catalyzes the rate-limiting step of sphingolipid synthesis, has been shown to affect raft association of both Gas1p and Pma1p (Bagnat *et al.*, 2000; Lee *et al.*, 2002). The observation that the *elo2*Δ mutant has a similar reduction in sphingolipid synthesis but is not synthetically lethal with *erg6*Δ indicates that reduced levels of sphingolipids cannot fully account for the defect observed in *elo3*Δ. Second, *elo3*Δ mutant cells contain IPC-C as their main sphingolipid species at the expense of the more complex mannosylated lipids. Whether a defect in head group maturation of sphingolipids could affect raft formation needs to be established. Third, the IPC-C species in the *elo3*Δ mutant contains a C22/C24 very-long-chain fatty acid instead of the natural C26 fatty acid. Biophysical studies indicate that the interaction of cholesterol with sphingomyelin is not affected by differences in acyl chain length (Ohvo-Rekila *et al.*, 2002). Phase separation of lipids in model membranes, however, is favored by the mismatch of the hydrophobic interaction surface of the interacting lipids (Silvius *et al.*, 1996). A simplified static model of the interaction of ergosterol with C26-substituted lipids, assuming interdigitation of the C26 acyl chain into the hydrophobic core of the opposing membrane leaflet (Slater and Huang, 1988; but see also McIntosh *et al.*, 1992), is illustrated in Figure 12. According to this model, shortening of the C26 acyl chain to C22 with the simultaneous removal of the C24 methyl group on ergosterol could result in significant alterations in the hydrophobic core of the membrane that could affect the domain-forming properties of the respective membrane.

Taken together, the observation of a genetic interaction between mutations in genes required for fungal specific lipid modifications of sphingolipids and sterols provides a new means to study the function, biogenesis, and regulation of raft structures in vivo, using genetic approaches unique to yeast.

ACKNOWLEDGMENTS

We thank A. Conzelmann, G. Daum, J. Gerst, C. Holm, G. Loison, F. Portillo, H. Riezman, M. Rose, and M. Snyder for generously pro-

viding plasmids, yeast strains, or antibodies; P. Seiser for initial help with the synthetic lethal screen; and S. Rosenberger, D. Gaug, and S. Reiner for help in the revision phase of this manuscript. This work was supported by the Austrian Science Found (P13767 and P15210 to R.S.). R.S. acknowledges receipt of a professorial award from the Swiss National Science Foundation.

REFERENCES

Bagnat, M., Chang, A., and Simons, K. (2001). Plasma membrane proton ATPase Pma1p requires raft association for surface delivery in yeast. Mol. Biol. Cell *12*, 4129–4138.

Bagnat, M., Keranen, S., Shevchenko, A., and Simons, K. (2000). Lipid rafts function in biosynthetic delivery of proteins to the cell surface in yeast. Proc. Nat. Acad. Sci. USA *97*, 3254–3259.

Brown, D.A., and London, E. (2000). Structure and function of sphingolipid- and cholesterol-rich membrane rafts. J. Biol. Chem. *275*, 17221–17224.

Brown, D.A., and Rose, J.K. (1992). Sorting of GPI-anchored proteins to glycolipid-enriched membrane subdomains during transport to the apical cell surface. Cell *68*, 533–544.

Burns, N., Grimwade, B., Ross-Macdonald, P.B., Choi, E.Y., Finberg, K., Roeder, G.S., and Snyder, M. (1994). Large-scale analysis of gene expression, protein localization, and gene disruption in *Saccharomyces cerevisiae*. Genes Dev. *8*, 1087–1105.

Christianson, T.W., Sikorski, R.S., Dante, M., Shero, J.H., and Hieter, P. (1992). Multifunctional yeast high-copy-number shuttle vectors. Gene *110*, 119–122.

Crowley, J.H., Smith, S.J., Leak, F.W., and Parks, L.W. (1996). Aerobic isolation of an *ERG24* null mutant of *Saccharomyces cerevisiae*. J. Bacteriol. *178*, 2991–2993.

Dahl, C., Biemann, H.P., and Dahl, J. (1987). A protein kinase antigenically related to pp60v-src possibly involved in yeast cell cycle control: positive in vivo regulation by sterol. Proc. Natl. Acad. Sci. USA *84*, 4012–4016.

David, D., Sundarababu, S., and Gerst, J.E. (1998). Involvement of long chain fatty acid elongation in the trafficking of secretory vesicles in yeast. J. Cell Biol. *143*, 1167–1182.

Dickson, R.C. (1998). Sphingolipid functions in *Saccharomyces cerevisiae*: comparison to mammals. Annu. Rev. Biochem. *67*, 27–48.

Fankhauser, C., and Conzelmann, A. (1991). Purification, biosynthesis and cellular localization of a major 125-kDa glycophosphatidylinositol-anchored membrane glycoprotein of *Saccharomyces cerevisiae*. Eur. J. Biochem. *195*, 439–448.

Ferreira, T., Mason, A.B., Pypaert, M., Allen, K.E., and Slayman, C. (2002). Quality control in the yeast secretory pathway. J. Biol. Chem. *277*, 21027–21040.

Funato, K., and Riezman, H. (2001). Vesicular and nonvesicular transport of ceramide from ER to the Golgi apparatus in yeast. J. Cell Biol. *155*, 949–959.

Gaber, R.F., Copple, D.M., Kennedy, B.K., Vidal, M., and Bard, M. (1989). The yeast gene *ERG6* is required for normal membrane function but is not essential for biosynthesis of the cell-cycle-sparking sterol. Mol. Cell. Biol. *9*, 3447–3456.

García-Arranz, M., Maldonado, A.M., Mazón, M.J., and Portillo, F. (1994). Transcriptional control of yeast plasma membrane H^+-ATPase by glucose. J. Biol. Chem. *269*, 18076–18082.

Goldstein, A., and Lampen, J.O. (1975). Beta-D-fructofuranoside fructohydrolase from yeast. Methods Enzymol. *42*, 504–511.

Gong, X., and Chang, A. (2001). A mutant plasma membrane ATPase, Pma1–10, is defective in stability at the yeast cell surface. Proc. Natl. Acad. Sci. USA *98*, 9104–9109.

Gu, M., Kerwin, J.L., Watts, J.D., and Aebersold, R. (1997). Ceramide profiling of complex lipid mixtures by electrospray ionization mass spectrometry. Anal. Biochem. *244*, 347–356.

Hannun, Y.A., and Luberto, C. (2000). Ceramide in the eukaryotic stress response. Trends Cell Biol. *10*, 73–80.

Hechtberger, P., Zinser, E., Saf, R., Hummel, K., Paltauf, F., and Daum, G. (1994). Characterization, quantification and subcellular localization of inositol-containing sphingolipids of the yeast *Saccharomyces cerevisiae.* Eur. J. Biochem. *225*, 641–649.

Jones, E. (1991). Three proteolytic systems in the yeast *Saccharomyces cerevisiae*. J. Biol. Chem. *266*, 7963–7966.

Kranz, J.E., and Holm, C. (1990). Cloning by function: An alternative approach for identifying yeast homologs of genes from other organisms. Proc. Natl. Acad. Sci. USA *87*, 6629–6633.

Ladevèze, V., Marcireau, C., Delourme, D., and Karst, F. (1993). General resistance to sterol biosynthesis inhibitors in *Saccharomyces cerevisiae*. Lipids *28*, 907–912.

Lange, Y., Swaisgood, M.H., Ramos, B.V., and Steck, T.L. (1989). Plasma membranes contain half the phospholipid and 90% of the cholesterol and sphingomyelin in cultured fibroblasts. J. Biol. Chem. *264*, 3786–3793.

Lee, M.C.S., Hamamoto, S., and Schekman, R. (2002). Ceramide biosynthesis is required for the formation of the oligomeric H^+-ATPase Pma1p in the yeast endoplasmic reticulum. J. Biol. Chem. *277*, 22395–22401.

Lees, N.D., Bard, M., and Kirsch, D.R. (1999). Biochemistry and molecular biology of sterol synthesis in *Saccharomyces cerevisiae*. Crit. Rev. Biochem. Mol. Biol. *34*, 33–47.

Levine, T.P., Wiggins, C.A., and Munro, S. (2000). Inositol phosphorylceramide synthase is located in the Golgi apparatus of *Saccharomyces cerevisiae*. Mol. Biol. Cell *11*, 2267–2281.

Longtine, M.S., McKenzie, A., 3rd, Demarini, D.J., Shah, N.G., Wach, A., Brachat, A., Philippsen, P., and Pringle, J.R. (1998). Additional modules for versatile and economical PCR-based gene deletion and modification in *Saccharomyces cerevisiae*. Yeast *14*, 953–961.

McIntosh, T.J., Simon, S.A., Needham, D., and Huang, C.H. (1992). Structure and cohesive properties of sphingomyelin/cholesterol bilayers. Biochemistry *31*, 2012–2020.

Muniz, M., and Riezman, H. (2000). Intracellular transport of GPI-anchored proteins. EMBO J. *19*, 10–15.

Munn, A.L., HeesePeck, A., Stevenson, B.J., Pichler, H., and Riezman, H. (1999). Specific sterols required for the internalization step of endocytosis in yeast. Mol. Biol. Cell *10*, 3943–3957.

Novick, P., and Schekman, R. (1979). Secretion and cell-surface growth are blocked in a temperature-sensitive mutant of *Saccharomyces cerevisiae*. Proc. Natl. Acad. Sci. USA *76*, 1858–1862.

Oh, C.S., Toke, D.A., Mandala, S., and Martin, C.E. (1997). *ELO2* and *ELO3*, homologues of the *Saccharomyces cerevisiae ELO1* gene, function in fatty acid elongation and are required for sphingolipid formation. J. Biol. Chem. *272*, 17376–17384.

Ohvo-Rekila, H., Ramstedt, B., Leppimaki, P., and Slotte, J.P. (2002). Cholesterol interactions with phospholipids in membranes. Prog. Lipid Res. *41*, 66–97.

Parks, L.W., Crowley, J.H., Leak, F.W., Smith, S.J., and Tomeo, M.E. (1999). Use of sterol mutants as probes for sterol functions in the yeast *Saccharomyces cerevisiae*. Crit. Rev. Biochem. Mol. Biol. *34*, 399–404.

Patton, J.L., and Lester, R.L. (1991). The phosphoinositol sphingolipids of *Saccharomyces cerevisiae* are highly localized in the plasma membrane. J. Bacteriol. *173*, 3101–3108.

Quail, M.A., and Kelly, S.L. (1996). The extraction and analysis of sterols from yeast. Methods Mol. Biol. *53*, 123–131.

Raths, S., Rohrer, J., Crausaz, F., and Riezman, H. (1993). *end3* and *end4*: two mutants defective in receptor-mediated and fluid- phase endocytosis in *Saccharomyces cerevisiae*. J. Cell Biol. *120*, 55–65.

Reggiori, F., Canivenc-Gansel, E., and Conzelmann, A. (1997). Lipid remodeling leads to the introduction and exchange of defined ceramides on GPI proteins in the ER and Golgi of *Saccharomyces cerevisiae*. EMBO J. *16*, 3506–3518.

Rietveld, A., and Simons, K. (1998). The differential miscibility of lipids as the basis for the formation of functional membrane rafts. Biochem. Biophys. Res. Commun. *1376*, 467–479.

Rodriguez, R.J., and Parks, L.W. (1983). Structural and physiological features of sterols necessary to satisfy bulk membrane and sparking requirements in yeast sterol auxotrophs. Arch. Biochem. Biophys. *225*, 861–871.

Sankaram, M.B., and Thompson, T.E. (1990). Interaction of cholesterol with various glycerophospholipids and sphingomyelin. Biochemistry *29*, 10670–10675.

Schneiter, R. (1999). Brave little yeast, please guide us to Thebes: sphingolipid function in *S. cerevisiae*. Bioessays *21*, 1004–1010.

Schneiter, R. *et al.* (1999). Electrospray ionization tandem mass spectrometry (E.S.I-M.S/M.S) analysis of the lipid molecular species composition of yeast subcellular membranes reveals acyl chain-based sorting/remodeling of distinct molecular species en route to the plasma membrane. J. Cell Biol. *146*, 741–754.

Schroeder, R., London, E., and Brown, D. (1994). Interactions between saturated acyl chains confer detergent resistance on lipids and glycosylphosphatidylinositol (GPI)-anchored proteins: GPI-anchored proteins in liposomes and cells show similar behavior. Proc. Natl. Acad. Sci. USA *91*, 12130–12134.

Shah, N., and Klausner, R.D. (1993). Brefeldin A reversibly inhibits secretion in *Saccharomyces cerevisiae*. J. Biol. Chem. *268*, 5345–5348.

Sievi, E., Suntio, T., and Makarow, M. (2001). Proteolytic function of GPI-anchored plasma membrane protease Yps1p in the yeast vacuole and Golgi. Traffic *2*, 896–907.

Sikorski, R.S., and Hieter, P. (1989). A system of shuttle vectors and yeast host strains designed for efficient manipulation of DNA in *Saccharomyces cerevisiae*. Genetics *122*, 19–27.

Silve, S. *et al.* (1996). The immunosuppressant S.R31747 blocks cell proliferation by inhibiting a steroid isomerase in *Saccharomyces cerevisiae*. Mol. Cell. Biol. *16*, 2719–2727.

Silvius, J.R., delGiudice, D., and Lafleur, M. (1996). Cholesterol at different bilayer concentrations can promote or antagonize lateral segregation of phospholipids of differing acyl chain length. Biochemistry *35*, 15198–15208.

Simons, K., and Ikonen, E. (1997). Functional rafts in cell membranes. Nature *387*, 569–572.

Sipos, G., Reggiori, F., Vionnet, C., and Conzelmann, A. (1997). Alternative lipid remodelling pathways for glycosylphosphatidylinositol membrane anchors in *Saccharomyces cerevisiae*. EMBO J. *16*, 3494–3505.

Slater, J.L., and Huang, C.H. (1988). Interdigitated bilayer membranes. Prog. Lipid Res. *27*, 325–359.

Sütterlin, C., Doering, T.L., Schimmoller, F., Schroder, S., and Riezman, H. (1997). Specific requirements for the ER to Golgi transport of GPI-anchored proteins in yeast. J. Cell Sci. *110*, 2703–2714.

Swain, E., Baudry, K., Stukey, J., McDonough, V., Germann, M., and Nickels, J.T., Jr. (2002). Sterol-dependent regulation of sphingolipid metabolism in *Saccharomyces cerevisiae*. J. Biol. Chem. *277*, 26177–26184.

Wach, A., Brachat, A., Pohlmann, R., and Philippsen, P. (1994). New heterologous modules for classical or PCR-based gene disruptions in *Saccharomyces cerevisiae*. Yeast *10*, 1793–1808.

Winston, F., Dollard, C., and Ricupero-Hovasse, S.L. (1995). Construction of a set of convenient *Saccharomyces cerevisiae* strains that are isogenic to S288C. Yeast *11*, 53–55.

Winzeler, E.A. *et al.* (1999). Functional characterization of the *S. cerevisiae* genome by gene deletion and parallel analysis. Science *285*, 901–906.

Xu, X., Bittman, R., Duportail, G., Heissler, D., Vilcheze, C., and London, E. (2001). Effect of the structure of natural sterols and sphingolipids on the formation of ordered sphingolipid/sterol domains (rafts). Comparison of cholesterol to plant, fungal, and disease-associated sterols and comparison of sphingomyelin, cerebrosides, and ceramide. J. Biol. Chem. *276*, 33540–33546.